CFD modeling of slag fuming, with focus on freeze-lining formation

C.M.G. Rodrigues[1], M. Wu[1], M. Chintinne[2], A. Ishmurzin[3], G. Hackl[3], N. Voller[4], A. Ludwig[1] and A. Kharicha[1]

1. Montanuniversity of Leoben, 8700 Leoben, Austria. christian.gomes-rodrigues@unileoben.ac.at
2. Aurubis-Beerse, 2340 Beerse, Belgium.
3. RHI Magnesita, 8700 Leoben, Austria.
4. RHI Magnesita, 1120 Wien, Austria.

Keywords: fuming furnace, freeze lining, CFD simulation, VOF model, mixture continuum model

ABSTRACT

Slag fuming (SF) is a critical process for recycling zinc-containing slags, but the corrosive nature of molten slag poses challenges to the reactor durability. The freeze-lining (FL) technique offers a solution by forming a protective layer on the reactor wall. It requires intensive cooling using water-cooled jackets, which can stabilize the FL while compromising the energy efficiency of the process.

This study presents a CFD-based model to optimize the SF process by considering FL formation and its impact on heat transfer and reactor wall temperature. A volume-of-fluid (VOF) model is coupled with a mixture continuum (MC) solidification model to capture the intricate multiphase flow dynamics within the SF furnace. Two FL types are considered: FL solidifying on the reactor wall in the slag bath region, and FL solidifying on the reactor wall in the freeboard region. The FL of the first type forms when the slag temperature drops below liquidus temperature. The FL of the second type only forms when a splash-induced slag droplet collides with the freeboard wall and solidifies. A series of splashing events are necessary to coat the freeboard wall.

The simulation was run until a global energy balance was reached. This means that the heat losses from the water-cooled jacket, bottom wall, outlet and fuming balance the heat gains from the hot gas injected through the submerged plasma torches. The increase in FL thickness, due to its low thermal conductivity, reduces the heat losses through the reactor walls. The calculated FL thickness and heat fluxes were in good agreement with industrial data, validating the model's credibility.

The simulation results provided valuable insights into the fuming process, including slag bath temperature evolution, slag splashing dynamics, FL formation patterns, local heat fluxes through the reactor wall, and overall energy balance. These findings can inform process optimization strategies to enhance the energy efficiency and sustainability of SF operations.

The current authors have built a prior version of the model framework, and applied it to simulate FL formation in an electric smelting furnace (ESF). The results from both the ESF and the current SF highlight the applicability of such model framework to a range of industrial processes involving FL formation. This model framework can ultimately contribute to more energy-efficient and sustainable industrial operations.

INTRODUCTION

Zinc, the world's fourth most consumed metal, plays a crucial role in various industries and in our daily life. Its annual global refined production surpasses 13.6 million tonnes (Kania and Saternus, 2023). However, the limited natural sources raise concerns about the sustainability of zinc production and its potential environmental impact. To address these challenges, a paradigm shift is needed, i.e. to prioritize zinc recycling. The recycling rate of 15-35% for zinc is low (Worell and Reuter, 2014). Over the past decades, various technologies have emerged to recover zinc from slags and produce clean slags for value-added applications (Kaya et al., 2020). One such process is the SF technology. It involves injecting coal and gas into molten slag to convert zinc oxides into metallic vapor (Verscheure et al., 2005). Optimal fuming rates can be achieved at high slag temperatures. However, the high temperature would rapidly erode furnace reactors or refractory linings, reducing their

lifespan and increasing maintenance costs. To overcome this problem, modern SF furnaces often incorporate water-cooled jackets. These jackets promote FL formation, a solidified layer of slag that acts as a protective barrier against the corrosive effects of molten slag (Verscheure et al., 2006).

FL formation has been extensively studied through both laboratory experiments and numerical models. Laboratory experiments have shown that the microstructure and thickness of FLs are determined by the solidification kinetics and slag chemistry (Campfort et al., 2009a, 2009b), and the FL front is influenced by the fluid flow (Fallah-Mehrjardi et al., 2013a, 2013b, Nagraj et al., 2021). Modeling studies have also provided valuable insights into the governing mechanisms of FL formation. The early models had limited applicability due to their simplicity (Wei et al., 1997; Campbell et al., 2002), but numerical advancements over time have made models more capable of capturing the intricate mechanisms involved in FL formation (Guevara et al., 2007, 2011, Feng et al., 2019).

Recently, the current authors developed a comprehensive model framework for simulating FL formation, extending the capabilities of previous numerical models by coupling FL formation with the flow dynamics, mass transfer processes, and energy transport mechanisms. The model framework was applied to an ESF and accounted for the intricate energy balance between the electrode joule heating, matte production, FL formation or melting, feed presence, and the cooling system (Rodrigues et al., 2023). This comprehensive representation of the system's energy balance was found crucial to accurately predict the FL layer behaviour. To further validate and expand the applicability of the model framework, the current authors applied it to the batch-type plasma-driven SF furnace operated at Aurubis-Beerse (Rodrigues et al., 2024). For an accurate representation of the multiphase flow with sharp interfaces between the gas and slag phases, the VOF formulation was integrated into the model framework. FL formation in both slag bath and freeboard was successfully captured. The simulation results were compared against industrial data, and demonstrated a remarkable agreement that validated the model's accuracy.

This paper continues the authors' previous research on FL formation in the batch-type plasma-driven SF furnace. The primary focus of this work is to delve into the process dynamics, from furnace start-up to the establishment of a global net energy balance. The evolution of FL formation, slag temperature, and heat flux patterns are analysed.

MODEL DESCRIPTION

Table 1 presents an overview of the model framework, which was described in detail in Rodrigues et al. (2023, 2024). Here, only an outline is provided. Three phases (or phase states) are considered: gas, liquid bulk slag, and solid slag (i.e. FL). The gas and the slag are captured with a VOF model. Their volume fractions add up to one ($\alpha_{\text{slag}} + \alpha_{\text{gas}} = 1.0$). The conservation equations for continuity, momentum and energy are shown in Eq. (1-3). The sensible enthalpy is defined by $h = \int_{298.15}^{T} c_p dT$. Solidification occurs exclusively in the slag, which exists in two states (solid and liquid), and their volume fractions add up to one ($f_s + f_\ell = 1.0$). The solidification is solved with a mixture continuum (MC) model. The solidification path shown in Fig. 1 is used to calculate f_s as function of T. The source term S_H (Eq. 4) is the latent heat released/absorbed during solidification/re-melting. The drag term $\vec{S}_U$ (Eq. 5) is included in the momentum conservation equation to dampen the flow in the mushy zone. The term S_S is the energy sink associated with the fuming rate. Owing to commercial reasons, details about this source term are omitted.

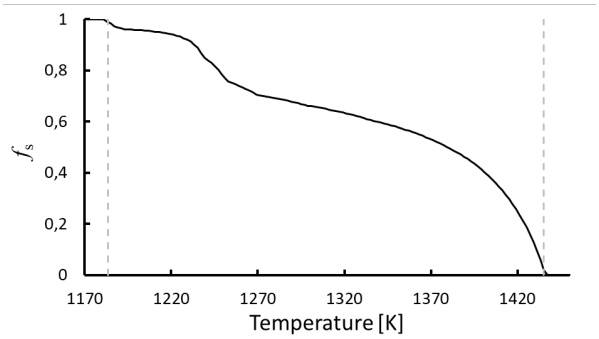

FIG 1 – Solidification path for the slag.

TABLE 1 – Model overview.

Conservation equations	
$\frac{\partial \alpha_{\text{slag}} \rho_{\text{slag}}}{\partial t} + \nabla \cdot (\alpha_{\text{slag}} \rho_{\text{slag}} \vec{u}_{\text{slag}}) = 0 \qquad \text{with } \alpha_{\text{slag}} + \alpha_{gas} = 1$	(1)
$\frac{\partial}{\partial t}(\rho \vec{u}) + \nabla \cdot (\rho \vec{u} \vec{u}) = \rho \vec{g} - \nabla p + \nabla (\mu \nabla \cdot \vec{u}) + \alpha_{\text{slag}} \vec{S}_{\text{U}}$	(2)
$\frac{\partial}{\partial t}(\rho h) + \nabla \cdot (\rho \vec{u} h) = \nabla \cdot (k_{\text{c}} \nabla T) + \alpha_{\text{slag}} S_{\text{H}} + \alpha_{\text{slag}} S_{\text{S}}$	(3)
Source terms	
$S_{\text{H}} = \rho_{\text{slag}} L_{\text{slag}} \frac{\partial f_{\text{s}}}{\partial t}$	(4)
$\vec{S}_{\text{U}} = -K_0 \frac{f_{\text{s}}^2}{(1 - f_{\text{s}})^3} \vec{u}_{\text{slag}}$	(5)

The simulation settings are summarized in Figure 2. Due to the large volume and the symmetry condition of the SF furnace, only one-third of the total furnace is considered. A mesh with 3.6 million cells is employed, with a local refinement near the wall (with 4 mm cells) to ensure adequate resolution of the FL layer. To effectively handle the complex flow dynamics near the furnace walls and the relatively high inlet gas velocity, a variable time stepping scheme between 10^{-5} and 10^{-4} seconds is employed. The computational domain is initialized with T_0 = 1473 K and a prescribed FL layer of 0.024 m on the reactor's inner walls in the freeboard region. This patched FL layer ensures that a global net energy balance can be established within a reasonable timeframe.

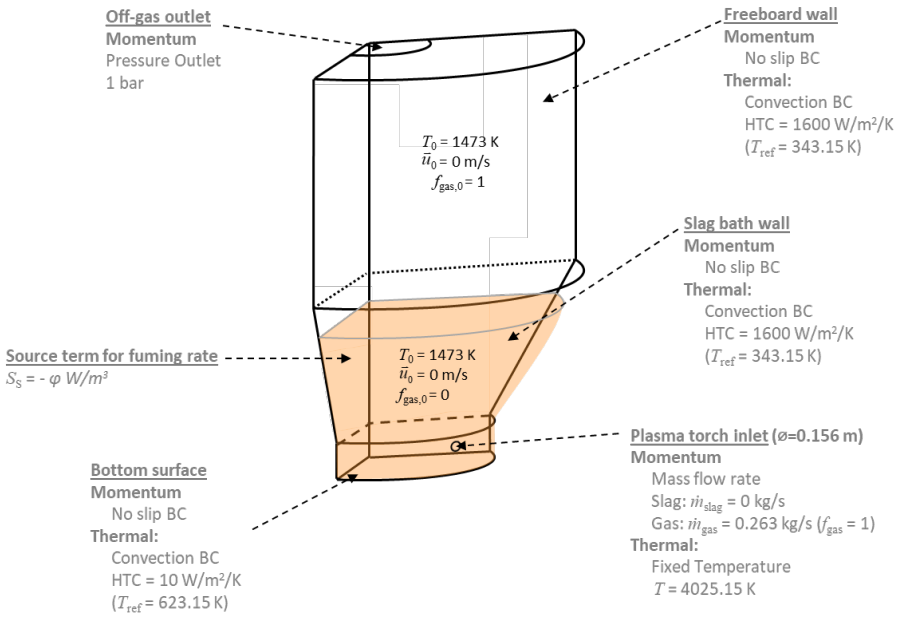

FIG 2 – Simulation settings for industrial SF furnace.

RESULTS

Figure 3 shows the temporal evolution of the slag fuming process, from a completely static slag bath with significant superheat to a quasi-steady state with global net energy balance. The first column presents a series of snapshots of the 3D iso-surface at the slag/gas interface, which highlights the dynamics behaviour of the slag splashing onto the freeboard surface. The colour scale represents the temperature distribution. The second and third columns show snapshots in a 2D vertical plane

of T and α_{slag} contours, respectively. The temperature contour demonstrates the gradual decline of superheat until the establishment of thermal equilibrium. The slag volume fraction contour is overlaid with streamlines to convey the dynamic behaviour of the flow both in the slag bath and in the freeboard. The fourth column shows snapshots of the 3D iso-surface depicting the thickness distribution of the FL layer on the reactor walls.

Early in the process (t = 30 s), slag splashing is widespread and intense, as evidenced by the high and wide range of splashing occurrences (Fig. 3 a1). This phenomenon stems from the high temperature (Fig. 3 b1) and low viscosity of the slag phase. However, the relatively large superheat of the molten slag impedes FL formation in the freeboard region. This is evident from the uniform grey colour in the freeboard region in Fig. 3 d1, which coincides with the thickness of the patched FL layer (2.4 cm). This indicates that no FL has formed on the freeboard surface. In contrast, in the slag bath region, where no patch was assumed, the FL has solidified to a maximum thickness of 0.4 cm, despite certain areas near the inlet remaining entirely devoid of FL.

At t = 100 s, the temperature of the slag bath remains elevated. The splashing events traversing the freeboard increase the temperature locally (Fig. 3 b2). Interestingly, slag flow is also quite dynamic within the slag bath, as indicated by the streamlines in Fig. 3 c2. This dynamic flow is crucial for distributing heat across the slag bath and enhancing slag fuming efficiency. No splash-induced FL formation occurs on the freeboard. In the slag bath region, the FL thickness starts to increase in certain areas to 0.8 cm.

At t = 150 s, the average slag bath temperature approaches 1445 K (Fig. 3 b3) and the first splash-induced FL formations emerge in the freeboard region (Fig. 3 d3). As a result, the FL thickness increases from 2.4 cm (assumed in the initial patch) to 3.0 cm in the darker areas. At this stage, FL formations primarily arise from splashing of individual slag droplets. This phenomenon can be attributed to the larger surface area-to-volume ratio, characteristic of smaller bodies, which expedites heat loss when the small slag droplet impacts on the freeboard surface. In contrast, larger bodies fail to reduce their temperature sufficiently to solidify upon impact and, instead, slide down the surface and merge with the bulk slag in the slag bath. In the slag bath region, the FL thickness increases to 1.8 cm, except in the region above the inlet, where the FL maintains a thickness of 1.3 cm due to the influence of the hot gas plumes generated by the submerged plasma torches (SPT).

At t = 180 s, the average slag bath temperature decreases to approximately 1439 K (Fig. 3 b4). This reduction in temperature significantly elevates the likelihood of FL formation in the freeboard region with each successive slag splashing/coating. For instance, in addition to the ongoing splashing event highlighted in Fig. 3 a4, a distinct slag layer is visible coating the wall at a temperature lower than the bulk molten slag (as indicated by the green colour on the freeboard surface, contrasting with the orange colour in the molten slag). Correspondingly, the FL layer covers a larger area, as demonstrated in Fig. 3 d4. Furthermore, the influence of slag splashing on gas flow dynamics becomes evident in the freeboard region (Fig. 3 c4). The streamlines become more chaotic but tend to align with the trajectories of the molten slag bodies, highlighting the direct impact of splashing on the gas flow patterns within the system.

At t = 220 s, a global net energy balance has been achieved in the simulation. Despite the transient nature of the flow dynamics beyond this stage, the overall energy balance persists in equilibrium over time. This means that a thermal equilibrium has been attained between the heat input (from the superheated slag bath and the injected hot gas), heat removal (by the cooling system, off-gas outlet, bottom surface, and fuming reaction), and latent heat (associated with melting or solidification). The average slag temperature stabilizes at approximately 1436.5 K (Fig. 3 b5), which is 1.4 K above the liquidus temperature. The splashing-induced FL formation continues to expand its coverage area in the freeboard (Fig. 3 d5). However, it is predominantly concentrated near the centreline of the domain, with the top corners of the reactor remaining untouched by splashing. This concentration pattern is attributed to the chosen gas density in the model, as discussed by Rodrigues et al. (2024). The majority of the predicted FL thickness measures 3.0 cm, with some small areas appearing near the interface between the slag bath and the freeboard reaching 3.6 cm. This means that a newly created splash-induced FL layer was formed on top of a pre-existing FL layer. In the slag bath, the FL thickness increases to 3.0 cm, except in the vicinity of the inlet and along the vertical path near the surface, where the FL thickness is affected by the presence of the hot gas plumes.

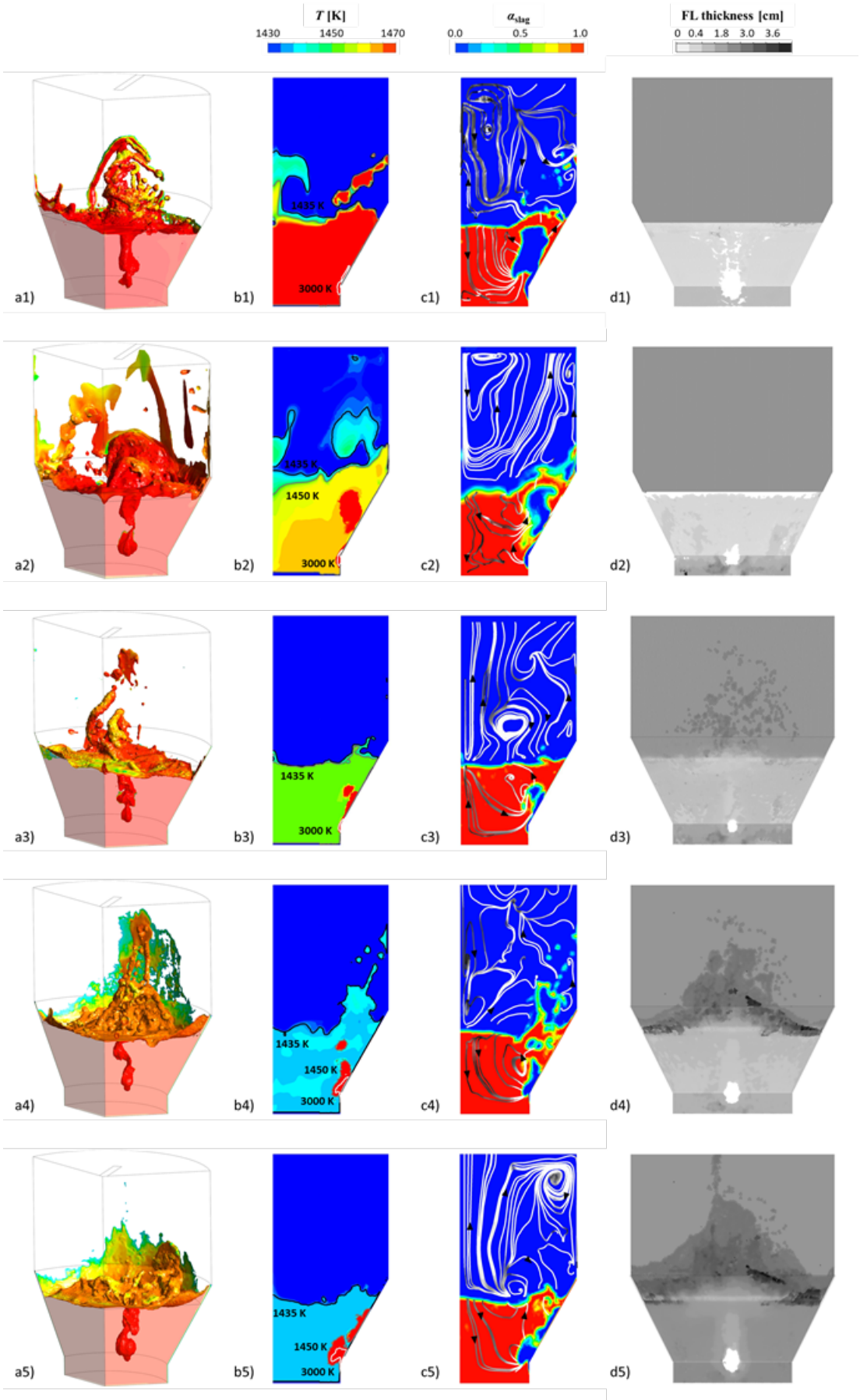

FIG 3 – Slag fuming process evolution at 1) t = 30 s, 2) t = 100 s, 3) t = 150 s, 4) t = 180 s, 5) t = 220 s. Simulation results for a) iso-surface at slag/gas interface with temperature contour, b) contour of T overlaid with isotherms in 2D vertical plane, c) contour of α_{slag} overlaid with velocity streamlines in 2D vertical plane, and d) distribution of FL thickness in grey scale on the furnace wall.

The final FL layer on the freeboard, shown in Fig. 3 d5, is limited by the computational time constraints of the simulation. However, the evolution of the FL layer demonstrates that the model can capture FL formation in the freeboard region and that its evolution is directly dependent on the splashing number and range during the SF process. The simulation results for FL thickness in the slag bath and in the coated freeboard agree well with the estimated average 3 cm FL layer reported in industrial data. After reaching a global net energy balance, heat fluxes on specific reactor surfaces were compared against the industrial furnace heat balance data. The error is analysed in Table 2, revealing a clear agreement between simulation results and industrial data.

TABLE 2 – Error percentage of heat fluxes on reactor walls after achieving a global net energy balance.

Heat fluxes [MW]	
Surfaces	**Error %**
Inlet	-0.4
Roof	-1.4
Walls	-0.4
Fuming reaction	-0.4

CONCLUSIONS

A CFD model framework has been developed to predict FL formation in a batch-type plasma-driven slag fuming furnace used for recycling Zn from slag. The FL is pivotal to protect the reactor walls and refractories from the corrosive molten slag and to act as an effective thermal barrier to enhance energy efficiency.

The model was successfully used to simulate FL evolution during the fuming process. The simulation results revealed a clear interplay between fluid flow, heat transfer, and FL formation. Prediction of critical phenomena, including slag splashing, wall coating, and freeze-lining formation, demonstrates the model's capability, providing valuable insights for a comprehensive understanding of the fuming process. Upon achieving a global net energy balance, the FL thickness and the heat fluxes through the main surfaces of the reactor agreed well with industrial data, validating the model's applicability in real-world scenarios.

The comprehensive understanding of fuming process dynamics facilitated by the model equips operators and engineers to make informed decisions, implement long-term targeted improvements, and optimize operational parameters for enhanced efficiency and energy conservation. The model has proven capable of being used in a wide range of other industrial applications where FL formation plays a significant role.

ACKNOWLEDGEMENTS

This study was supported by the Austrian Research Promotion Agency (FFG) under the framework of Bridge 1 program (MoSSoFreez Project, F0999888120). We thank Dr. Muxing Guo, Dr. Annelies Malfliet, and Dr. Zilong Qiu from KU Leuven, as well as Dr. Samant Nagraj from Umicore for their discussions and valuable inputs. Approval from Aurubis-Beerse to publish manuscript is also acknowledged.

REFERENCES

Campbell, A P, Pericleous, K A and Cross, M, 2002. Modelling of freeze layers and refractory wear in direct smelting processes in *Ironmaking conference*, pp. 479–491

Campforts, M, Jak, E, Blanpain, B and Wollants, P, 2009. Freeze-Lining Formation of a Synthetic Lead Slag: Part I. Microstructure Formation, *Metall. Mater. Trans. B*, 40:619–631.

Campforts, M, Jak, E, Blanpain, B and Wollants, P, 2009. Freeze-Lining Formation of a Synthetic Lead Slag: Part II. Thermal History, *Metall. Mater. Trans. B*, 40:632–642.

Fallah-Mehrjardi, A, Hayes, P C and Jak, E, 2013a. Investigation of Freeze-Linings in Copper-Containing Slag Systems: Part I. Preliminary Experiments, *Metall. Mater. Trans. B*, 44:534–548.

Fallah-Mehrjardi, A, Hayes, P C and Jak, E, 2013a. Investigation of Freeze-Linings in Copper-Containing Slag Systems: Part II. Mechanism of the Deposit Stabilization, *Metall. Mater. Trans. B*, 44:549–560.

Feng, Y, Gao, J, Feng, D and Zhang, X, 2019. Modeling of the Molten Blast Furnace Slag Particle Deposition on the Wall Including Phase Change and Heat Transfer, *Applied Energy*, 248:188–298.

Guevara, F, 2007. Study of slag freezing in metallurgical furnaces, PhD thesis, McMaster University.

Guevara, F and Irons, G, 2011. Simulation of slag freeze layer formation: Part II. Numerical study, *Metall. Mater. Trans. B*, 42:652–663.

Kania, H and Saternus, M, 2023. Evaluation and Current State of Primary and Secondary Zinc Production—A Review, *Appl. Sci.*, 13(3):1–22.

Kaya, M, Hussaini, S and Kursunoglu, S, 2020. Hydrometallurgy, Critical review on secondary zinc resources and their recycling technologies, Hydrometallurgy, 195:105362.

Nagraj, S, Chintinne, M, Guo, M and Blanpain, B, 2022. Investigation of Bath/Freeze Lining Interface Temperature Based on the Rheology of the Slag, *JOM*, 74:274–282.

Rodrigues C M G, Wu, M, Ishmurzin, A, Hackl, G, Voller, N, Ludwig, A and Kharicha, A, 2023. Modeling Framework for the Simulation of an Electric Smelting Furnace Considering Freeze Lining Formation, *Metall. Mater. Trans. B*, 54:880–894.

Rodrigues C M G, Wu, M, Chintinne, M, Ishmurzin, A, Hackl, G, Voller, N, Ludwig, A and Kharicha, A, 2024 (in prep). Modeling freeze-lining formation: a case study in the slag fuming process.

Verscheure, K, Van Camp, M, Blanpain, B, Wollant, P, Hayes, P and Jak, E, 2005. Investigation of Zing Fuming Processes for the Treatment of Zinc-containing Residues in *John Floyd International Symposium*, pp. 137–250.

Verscheure, K, Kyllo, A, Filzwieser, A and Blanpain, B, 2006. Furnace cooling technology in pyrometallurgical processes in *Sohn International Symposium*, pp. 139–154.

Wei, C, Chen, J, Welch, B and Voller, V, 1997. Modeling of dynamic ledge heat transfer in *Light Metals*, pp. 309–316.

Worell, E and Reuter, M A, 2014. Handbook of Recycling: State-of-the-art for Practitioners, Analysts, and Scientists, pp. 113–124 (Elsevier: Oxford).